

# TIME-OF-FLIGHT IMAGING OF INDOOR SCENES WITH SCATTERING COMPENSATION

James Mure-Dubois and Heinz Hügli

University of Neuchâtel

Institute of Microtechnology, 2000 Neuchâtel, Switzerland

{james.mure-dubois, heinz.hugli}@unine.ch

**KEY WORDS:** time-of-flight, range imaging, scattering, deconvolution, real-time.

## ABSTRACT

3D images from time-of-flight cameras may suffer from false depth readings caused by light scattering. In order to reduce such scattering artifacts, a scattering compensation procedure is proposed. Assuming a space invariant point spread function as a model for the scattering leads to a solution in a form of a deconvolution scheme. The improvement brought by scattering compensation, as well as the computational cost involved are further discussed in this paper.

## 1 INTRODUCTION

TOF cameras rely on active illumination and measure range from the time needed for light to travel from the camera light source to the scene and back to the camera. Recent time-of-flight (TOF) cameras allow for real-time acquisition of range maps. For instance, the Swissranger SR-3000 camera has a 176x144 sensor, and supports continuous operation at 20 Hz [1]. The depth resolution can be better than 1 cm in favourable conditions: indoors, with no bright light sources in the field of view [2].

However, depth measurement can be degraded by secondary reflections occurring between the lens and the imager. This phenomenon is designated thereafter as scattering [3]. Range image degradation by scattering occurs mainly when the spread of depth imaged is wide. In that case, the signal from far objects (background) can be affected by scattering from foreground objects. This degradation of the depth image is a significant penalty in many applications, especially when background subtraction methods are employed [3]. For this reason, scattering must be suppressed, or at least reduced.

The problem of scattering compensation by image processing methods is first discussed. By using a formalism where the data acquired by the TOF camera is expressed as a two-dimensional complex signal, scattering can be modelled as a convolution operation on this signal. In that case, scattering compensation can be realized by applying an inverse filter on the 2D complex signal returned by the camera [4]. We will show that, due to the anisotropic nature of the scattering phenomenon, the degradation is more pronounced along sensor rows than along sensor columns, and the filter employed must be wide.

In this paper, we also discuss the suitability of the inverse filter approach for real-time operation. Straightforward two-dimensional filtering is prohibitively expensive, due to the large filter size. However, by restricting the expression of the inverse filter to a sum of separable gaussians, real-time performance can be attained. Moreover, using separable gaussians allows to account for the anisotropic behaviour of scattering, by using different standard deviations along sensor rows or columns. We emphasize that the processing time can be reduced by a factor close to 100 when using the separable sum of gaussians expression. The performance can be increased further by using optimized filtering functions available in commercial image processing libraries. The proposed implementation allows continuous operation at 10 Hz, which is high enough for many real-time range imaging applications.

Finally, we will briefly outline our strategy to reach 20Hz continuous operation and better performance. Since the processing time scales with the filter size, we are currently investigating inverse filter optimization, aiming for better scattering compensation, but also for lower filter size.

## 2 TIME-OF-FLIGHT IMAGING AND SCATTERING

### 2.1 Time-of-flight camera operation

State-of-the-art TOF cameras ([5],[6],[7]) are based on the continuous emission of a periodic signal. The frequency of modulation  $f$  of this signal is typically 20MHz. The periodic signal received at each pixel  $(i, j)$  of the camera sensor is described by its amplitude  $A(i, j)$  and its phase  $\varphi(i, j)$ , which can be expressed as a complex signal  $S(i, j)$ . The range  $r$  is directly proportional to the phase. With  $c$  as the speed of light, we have :

$$S(i, j) = A(i, j) \cdot e^{j\varphi(i, j)} \quad r(i, j) = \frac{c}{4\pi f} \cdot \varphi(i, j) \quad (1)$$

Figure 1 shows intensity images (captured with a standard CCD camera) of a simple example scene, which consists of a person standing in a room. An image of the scene background was also included, since background is important in the discussion of scattering effects. Figure 2 shows the range images  $r(i, j)$  obtained for this example scene. As mentioned above, those maps are obtained from the phase of the complex signal measured at each sensor pixel.

### 2.2 Scattering in time-of-flight cameras

The degradation caused by scattering in TOF range imaging is best illustrated by comparing the range images measured without and with a foreground object. Figure 3 shows the difference of the range images in fig.2. The expected result is an image with a single active region, namely the shape of the person introduced in the field of view. However, fig.3 shows that the range value was changed for many background pixels. From this point on, we will call *scattering* the effect that causes this difference between the expected result and the data measured by the TOF camera. The perturbation is clearly related to the foreground object. The depth difference is highest for sensor pixels next to the object, and gets weaker for pixels near the image edges. Moreover, scattering effects appear to be anisotropic: the effect is stronger for some regions in the image (e.g. the floor), and the perturbation is more pronounced along sensor rows than along sensor columns. Finally, it is important to note that the reach of scattering is large : the entire image is affected, while the source of scattering occupies a limited region in the center of the image.

## 3 SCATTERING MODEL

The main mechanism behind scattering artifacts is a parasitic optical coupling between distinct pixels [1]. This coupling is caused by unwanted reflections on the camera sensor and optics, as illustrated schematically in fig.4. Although the strength of this coupling is very low, the effect on the phase image read by the TOF camera can be significant. Let us denote by  $S(i, j)$  the ideal signal entering the camera device,  $S_{scat}(i, j)$  the scattering signal due to parasitic reflections. Assuming that scattering is an additive perturbation, we can define  $S_{meas}(i, j)$ , the signal measured by the sensor, as the sum of those two signals :

$$S_{meas}(i, j) = S(i, j) + S_{scat}(i, j) \quad (2)$$

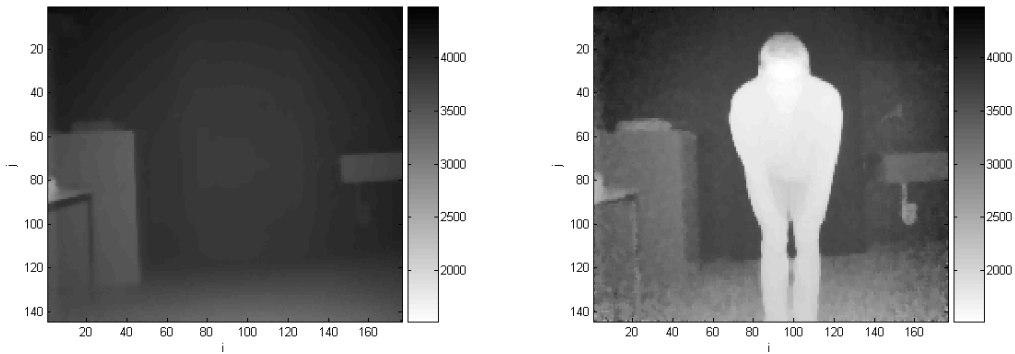
Moreover, by making the (strong) hypothesis that scattering is linear and space-invariant, we can express that scattering signal  $S_{scat}(i, j)$  as the result of the convolution of the ideal signal



(a) Indoor situation - Background

(b) Indoor situation with foreground object.

Figure 1: Intensity images of a typical indoor scene where TOF range imaging is affected by scattering.



(a) Background range image.

(b) Range image with foreground.

Figure 2: Illustration of TOF range imaging (Range scale in mm).

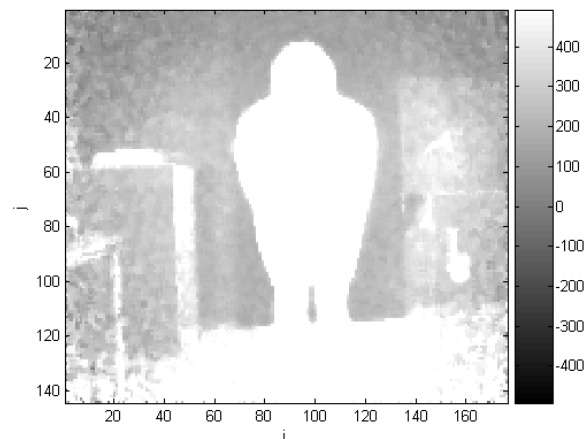


Figure 3: Range image difference (Range scale in mm, values out of range are clipped).

with a scattering point spread function (PSF)  $\Delta h(i, j)$ , i.e.  $S_{scat}(i, j) = S(i, j) * * \Delta h(i, j)$ . If we define  $\mathbf{h}_0$  as the neutral element with respect to convolution, we can express equation 2 with a convolution operation :

$$S_{meas}(i, j) = S(i, j) * *(h_0(i, j) + \Delta h(i, j)) = S(i, j) * * h(i, j) \quad (3)$$

where  $\mathbf{h} = \mathbf{h}_0 + \Delta \mathbf{h}$  is interpreted as a camera point spread function including scattering coupling.

This description is sufficient to adequately model the behaviour observed in section 2.2: having scattering effects weaken for pixels far away from the perturbation can be expressed by requiring that the scattering point spread function  $\Delta h(i, j)$  falls to 0 for elements (i,j) far from the origin; the different sensitivities to scattering observed for different regions can be understood as the consequence of the large span of amplitudes for the complex signals involved; finally, the asymmetry between sensor rows and columns can be described by an anisotropic PSF  $\Delta \mathbf{h}$ .

## 4 SCATTERING COMPENSATION

### 4.1 Goal of scattering compensation

The goal of scattering compensation is to recover  $\mathbf{S}$ , based on the signal  $\mathbf{S}_{meas}$  returned by the camera. This operation can be described as a blind deconvolution on a complex signal. Moreover, to be interesting in a practical application, the complexity of the compensation method used should be low enough to allow for real-time processing. Therefore, rather than trying to solve the blind deconvolution problem, we will assume the existence of an inverse filter, and make additional hypothesis on its form in order to allow for a real-time implementation.

### 4.2 Inverse filter for deconvolution

In the following discussion, we call  $\mathbf{I}$  the inverse filter which performs the deconvolution, that is :  $\mathbf{S} = \mathbf{S}_{meas} * * \mathbf{I}$ . The inverse filter can be rewritten as  $\mathbf{I} = \mathbf{h}_0 - \Delta \mathbf{I}$ , where  $\mathbf{h}_0$  is the neutral PSF with respect to convolution and  $\Delta \mathbf{I}$  is interpreted as the inverse scattering PSF. By identification in eq. 2, we have  $\mathbf{S}_{scat} = \mathbf{S}_{meas} * * \Delta \mathbf{I}$ . Scattering compensation can be performed if an accurate expression of  $\Delta \mathbf{I}$  is known, since we have :

$$\mathbf{S} = \mathbf{S}_{meas} - \mathbf{S}_{meas} * * \Delta \mathbf{I} \quad (4)$$

### 4.3 Inverse scattering PSF model

The expression for the inverse scattering PSF  $\Delta \mathbf{I}$  must be found to perform scattering compensation. Finding an exact solution to this problem is formally equivalent to solving the blind deconvolution problem for a complex 2D signal. As mentioned above, this approach is too complex in our application. To overcome this difficulty, we propose to use an approximate inverse scattering PSF  $\hat{\Delta \mathbf{I}}$ , which can then be iteratively updated, either through empirical experimentation or following a more systematic optimization strategy.

The properties of the scattering phenomenon can be used to describe the properties required for the inverse scattering PSF. First, since the reach of scattering is large, the extent of the inverse scattering PSF must also be large. This is a critical experimental problem: if the extent of the PSF is for example  $100 \times 100$ , the model for the inverse scattering can have as many as 10000 independent parameters. Unfortunately, a model with such a high count of parameters would be impossible to update systematically. To overcome this difficulty, the inverse scattering PSF  $\Delta \mathbf{I}$  can be modeled as a weighed sum of separable gaussian kernels of different standard deviation.

$$\hat{\Delta I}(i, j) = \sum_{k=1}^G w(k) \cdot I_h(i, k) \cdot I_v(j, k) \quad (5)$$

where :

- $\mathbf{I}_h$  is a 1D horizontal gaussian kernel ( $\in \mathbb{R}$ ):  $I_h(i, k) = \frac{1}{\sqrt{2\pi\sigma_h(k)}} e^{-\frac{i^2}{2\sigma_h^2(k)}}$
- $\mathbf{I}_v$  is a 1D vertical gaussian kernel ( $\in \mathbb{R}$ ):  $I_v(j, k) = \frac{1}{\sqrt{2\pi\sigma_v(k)}} e^{-\frac{j^2}{2\sigma_v^2(k)}}$
- $w(k)$  is a scalar ( $\in \mathbb{R}$ ) weight.

This choice is motivated by four main advantages :

- The weighted sum of gaussian allows to describe a large kernel with a small set of parameters.
- The asymmetry between sensor rows and columns can be modeled by choosing different standard deviation for vertical and horizontal kernels.
- The 2D filtering operation with  $\hat{\Delta}\mathbf{I}$  can be performed as a cascade of 1D convolutions for separable gaussian kernels. This is a significant reduction in algorithm complexity for large kernel sizes.
- The choice of gaussian kernels ensures that the inverse scattering PSF falls to 0 for large  $(i, j)$ .

## 5 PERFORMANCE OF COMPENSATION

The most critical aspects to take into account when evaluating the performance of a scattering compensation algorithm are :

- The improvement of the resulting range image, when compared to the raw range image
- The processing time : one of the main advantages of TOF imaging when compared to other range imaging methods (stereo, laser scan, etc.) is the ability to provide range information at high frame rates. Scattering compensation should not compromise this advantage.

In this paper, we will only provide a qualitative discussion of the improvement in the range image. Figure 5 shows a comparison of range images with and without scattering compensation. For better readability, difference from background was also included. It is clearly visible that most of the scattering effects are attenuated when compensation is used. Some regions of the image, for which the difference was as high as 400 mm in the raw image now show a difference of less than 100 mm. More details on a quantitative evaluation of the improvement in the range image can be found in [8].

In the following, we will focus on processing time and real-time operation issues. The parameters for the inverse scattering PSF model used in our study are reported in Table 1. Those parameters were obtained through empirical experimentation, with a human expert manually updating the model parameters in order to achieve the best compensation result. This specific model involves three gaussians, one of which has a 1:2 aspect ratio. To reduce processing time, the size of the inverse scattering PSF was limited to  $160 \times 160$ . Nevertheless, convolving a  $176 \times 144$  image with an arbitrary PSF of this size involves more than  $10^9$  multiplications. Using a sum of separable gaussians allows to reduce the number of multiplications required to less than  $5 \cdot 10^7$ .

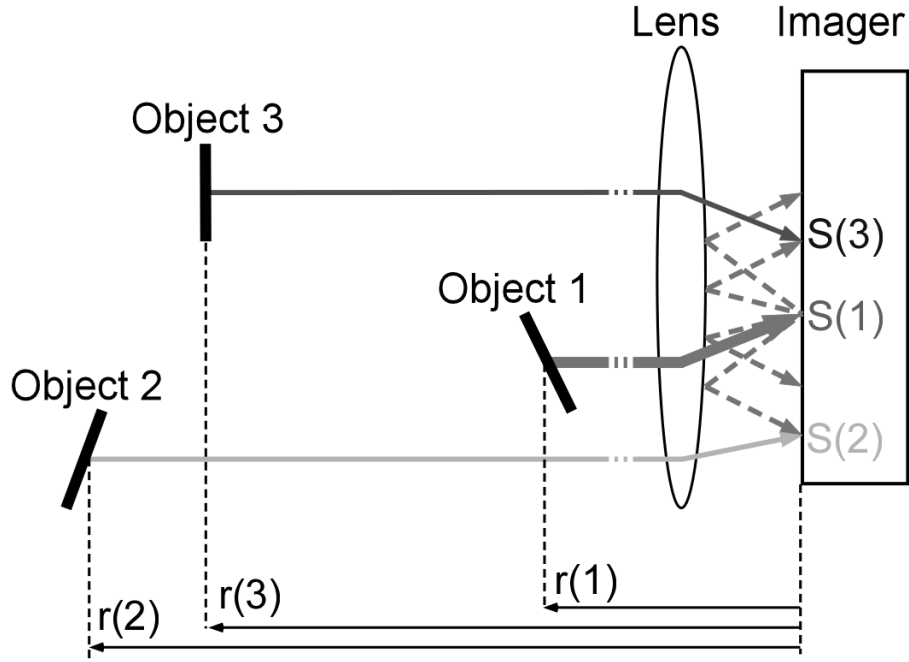


Figure 4: Light scattering in TOF camera .

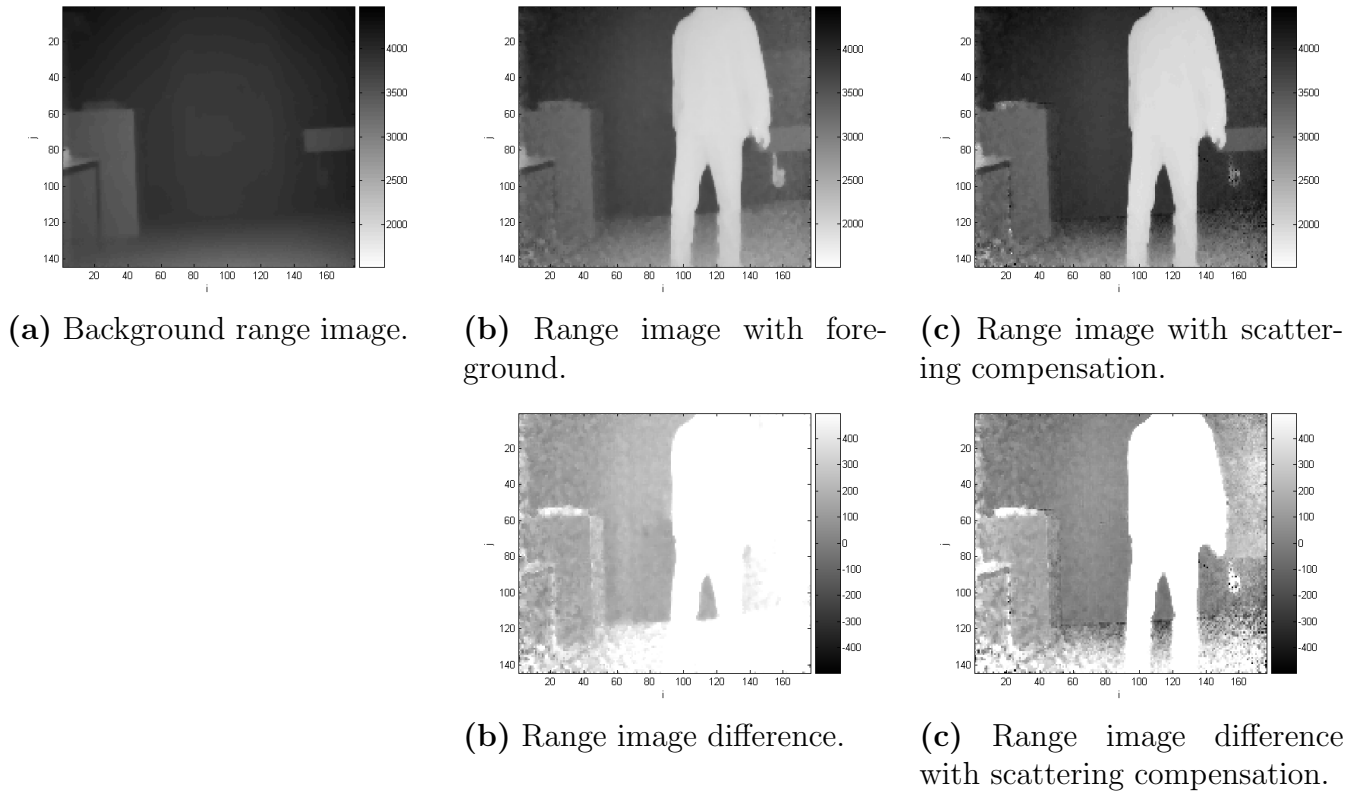


Figure 5: Illustration of scattering compensation results (Range scale in mm).

$k$	$\sigma_h$	$\sigma_v$	$w$
1	32	64	0.1000
2	48	48	0.0700
3	64	64	0.1800

Table 1: Parameters for the inverse scattering PSF used in scattering compensation experiments

Convolution method	Processing time	3D frame rate
full 2D	46.0 s	0.02 fps
separated	0.460 s	2 fps
separated (IPL)	0.085 s	10 fps

Table 2: Processing time and resulting frame rate for different convolution implementations

A software implementation of scattering compensation was developed. For comparison purposes, the software included three convolution implementations: a full 2D convolution (supporting an arbitrary PSF), a separable convolution (for PSF expressed as sum of separable gaussians) and a separable convolution using an optimized image processing library (IPL 2.5). Table 2 presents the typical processing time for each implementation, along with the continuous operation 3D frame rate when scattering compensation is enabled. Those values were obtained with a single-core, 3.2GHz Pentium 4 processor. The results clearly show that the general 2D convolution is prohibitively expensive, and can not be employed in a real-time application. Using a separated convolution approach allows to perform scattering compensation in real-time. Moreover, using an optimized library allows continuous operation at 10 fps.

## 6 CONCLUSION

In this paper, the degradation of the range image caused by scattering in a time-of-flight camera was presented. Based on the observed properties of the scattering phenomenon, a simple scattering model was introduced. This model was used to formulate scattering compensation as a blind deconvolution problem. An approximate solution to this problem was proposed in the form of an inverse filter, involving an inverse scattering PSF. A restriction of this PSF to a sum of separable gaussian kernels was introduced in order to reduce computation cost for the scattering compensation process. Qualitative results of the implemented scattering compensation algorithm were presented. A comparison of the processing time involved for three different implementations of the convolution operation was performed. The results show that the limitation of the inverse scattering PSF to a sum of separable gaussians is necessary for real-time operation. Moreover, it was shown that the proposed method allows for 10 fps continuous operation when using an optimized library for convolution operations.

Work is currently in progress to develop an automatic updating scheme for the inverse scattering parameters. This new development is expected to yield better scattering compensation results, both in terms of range image quality and in terms of computation speed.

## ACKNOWLEDGEMENTS

This work was supported by the Swiss Federal Innovation Promotion Agency KTI/CTI (Project no. 7719.1 ESPP-ES).

## REFERENCES

- [1] CSEM. Swissranger SR-3000 manual v1.02, June 2006. <http://www.swissranger.ch/customer>.
- [2] T. Kahlmann, F. Remondino, and H. Ingensand. Calibration for Increased Accuracy of the Range Imaging Camera SwissRanger. In *Proc. of the ISPRS Com. V Symposium*, pages 136–141. ISPRS, sep 2006.

- 
- [3] N. Santrac, G. Friedland, and R. Rojas. High Resolution Segmentation with a Time-of-flight 3D-Camera using the Example of a Lecture Scene, September 2006. Technical report, available from: <http://www.inf.fu-berlin.de/inst/ag-ki/eng/index.html>.
  - [4] R. C. Puetter, T. R. Gosnell, and A. Yahil. Digital Image Reconstruction: Deblurring and Denoising. *Annual Review of Astronomy and Astrophysics*, 43:139–194, September 2005.
  - [5] CSEM. Swissranger, 2006. <http://www.swissranger.ch>.
  - [6] PMD Technologies. Pmdvision, 2006. [http://www.pmdtec.com/e\\_index.htm](http://www.pmdtec.com/e_index.htm).
  - [7] Canesta Inc. Canestavision, 2006. <http://www.canesta.com/index.htm>.
  - [8] J. Mure-Dubois and H. Hügli. Real-time scattering compensation for time-of-flight camera. In *Proc. of the ICVS 2007*. ICVS, Feb 2007.